Interactive Dynamic Airspace Sectorization through Human-in-the-Loop Optimization

Clark Borst
Section Control & Simulation
Faculty of Aerospace Engineering
Delft University of Technology
2629 HS Delft, The Netherlands
email: c.borst@tudelft.nl

***Abstract*—Dynamic Airspace Sectorization (DAS) is a key enabler for a sustainable future of Air Traffic Management (ATM). It allows the continuous adaptation of airspace boundaries to changing traffic, weather, and operational constraints. In contrast to existing fully automated DAS optimization approaches, this article argues for a human–AI collaborative approach that balances automation with human agency. A human-in-the-loop optimization framework with corresponding Human-Machine Interface is proposed based on the Covariance Matrix Adaptation Evolution Strategy (CMA-ES). By integrating interactive and preference-guided search, the system allows airspace designers to steer evolutionary optimization while it learns from labeled human preferences in real time. The work presented in this paper represents an ongoing research prototype that explores how human operators can meaningfully participate in and guide the optimization process, illustrating the potential of interactive approaches for DAS and similar optimization contexts. Future work will focus on conducting human-in-the-loop experiments using NAV Portugal operational experts to study how operators interact with the system, evaluate interaction efficiency, acceptance, and understanding, and benchmark the quality of the resulting sectorization solutions against state-of-the-art algorithmic approaches.**

***Keywords*—dynamic airspace sectorization; human-in-the-loop optimization; human-machine interface**

I. Introduction

Dynamic airspace sectorization (DAS) can be fundamentally framed as an optimization problem in which sector boundaries must be continuously adapted in response to evolving traffic patterns, operational demands, and external constraints [1]–[4]. The need for adaptive sectorization capabilities is further intensified by emerging operational challenges that demand increased flexibility in airspace design.

Climate adaptation and environmental considerations are becoming increasingly relevant, requiring support for the avoidance of contrail-sensitive areas, re-routing around shifting jet streams, and improved weather avoidance strategies in the context of climate change [5]. In parallel, human resource and communication constraints are reshaping operational requirements. Sector reconfiguration can help mitigate predicted controller shortages [6] by redistributing workload more effectively and can accommodate evolving communication infrastructures such as satellite-based VHF systems [7], where the availability of radio frequencies and channels is limited.

The main DAS objective is to generate sector configurations that remain geometrically manageable, operationally intuitive, and well suited for controller oversight while ensuring safe and efficient traffic handling. Within this framework, much of the existing literature and current practice in dynamic sectorization has focused predominantly on fully automated optimization approaches that aim to compute optimal sector configurations with minimal or no human participation (see [8] for an overview). While such methods can achieve mathematically efficient solutions, they often neglect the importance of human judgment, contextual interpretation, and operational nuance that are essential in safety-critical environments such as Air Traffic Management (ATM). In practice, sector configurations must remain transparent, explainable, and adaptable to situational factors that may not be fully captured in formal optimization models. Airspace designers require insight into why a particular sectorization is proposed, how constraints are satisfied or violated, and how adjustments affect air traffic controller (ATCO) taskload and coordination. The limited integration of human interaction in existing optimization-driven approaches therefore represents a significant gap: without meaningful human involvement and transparency, even technically optimal solutions may lack operational acceptability or trust [9]. Addressing this gap requires interactive sectorization methods that allow airspace designers to remain actively engaged in the optimization process, combining computational efficiency with explainability and human-centered control.

The main contribution of this work is the development and implementation of a human-in-the-loop optimization framework with Human–Machine Interface (HMI) that enable meaningful human participation in the DAS optimization process while maintaining transparency of the underlying optimization and domain-relevant constraints. The interface allows operators to explore candidate sectorizations, understand trade-offs between competing objectives, and guide the search toward more operationally acceptable solutions. This human-in-the-loop approach aligns with broader EASA and European regulatory principles on trustworthy human–AI

This work has been conducted within the AI4REALNET (AI for REAL-world NETwork operation) project (https://ai4realnet.eu/), which received funding from the European Union's Horizon Europe Research and Innovation programme under the Grant Agreement No 101119527, and from the Swiss State Secretariat for Education, Research and Innovation (SERI).

collaboration by ensuring transparency [10], meaningful human oversight [11], and shared responsibility in safety-critical decision-making.

II. Background

A. Dynamic Airspace Sectorization

Within DAS, generally two competing objectives must be jointly optimized. First, sectors should be configured so that the predicted ATCO taskload is evenly distributed, typically expressed by minimizing the standard deviation of taskload across sectors to ensure balanced cognitive demand and sustainable operational performance. Second, the number of inter-sector hand-offs must be minimized, as each transfer of aircraft between sectors introduces coordination workload and potential complexity; reducing hand-offs promotes more continuous, unfragmented airspace structures. These two objectives are inherently competing because achieving a more balanced workload often requires splitting traffic flows across multiple sectors, which can increase the number of sector boundary crossings and thus coordination demands. Effective dynamic sectorization therefore requires carefully balancing workload equity and coordination efficiency, using flexible boundary design mechanisms to adapt sector geometry while maintaining operationally acceptable.

In addition to the two competing objectives, candidate sectorizations must satisfy a set of geometric and procedural constraints [1]–[3]:

- *Minimum route segment length:* Routes within a sector must not be subdivided into very short segments, as these cause excessive controller handovers and communication workload.
- *Intersection avoidance near boundaries:* Route intersections should not occur too close to sector boundaries to prevent coordination issues and to maintain situation awareness.
- *Sector size and shape:* Each sector must be large enough to maintain safe separation minima and small enough to manage complexity efficiently.
- *Connectivity and continuity:* Sectors must remain contiguous and without holes; disconnected regions are operationally infeasible.

B. Related work

DAS has been extensively studied as a complex optimization problem using a wide range of algorithmic approaches to automatically generate sector configurations under geometric, traffic, and coordination constraints. A recent publication [8] provides a comprehensive overview of the various optimization techniques studied in this domain.

In general, Voronoi tessellation has frequently been adopted as a geometric foundation for sector design due to its ability to generate convex and contiguous regions that are computationally efficient to manipulate [1], [2], [4]. By adjusting generator points, Voronoi-based methods enable flexible adaptation of sector boundaries while preserving structural validity, and they have been used both as standalone sectorization mechanisms and as components within larger optimization frameworks.

Mixed-integer linear programming (MILP) formulations have also been applied to the sectorization problem [12], [13], enabling explicit representation of workload balancing, sector connectivity, and coordination constraints. These approaches provide mathematically rigorous optimization guarantees but often suffer from scalability challenges as problem size and constraint complexity increase. To address computational limitations and explore larger solution spaces, heuristic and metaheuristic methods such as genetic algorithms [14], evolutionary strategies [15] and hybrid approaches [16] have been widely investigated. These techniques can generate diverse candidate sectorizations and approximate near-optimal solutions, particularly in dynamic or stochastic traffic scenarios.

Clustering-based techniques constitute another important class of approaches, where traffic flows, waypoints, or airspace regions are grouped according to similarity in workload or spatial proximity. Methods based on k-means, spectral clustering, DBSCAN and graph partitioning have been used to derive sector boundaries that balance traffic demand while preserving flow continuity [17], [18].

While these algorithmic approaches have significantly advanced automated sectorization capabilities, most existing work emphasizes fully automated optimization, with comparatively limited attention given to interactive, human-in-the-loop sector design and explainability in safety-critical operational contexts.

III. Human-in-the-Loop Optimization

This section introduces the proposed human-in-the-loop optimization framework, beginning with an overview of the underlying mathematical models, followed by a description of the human–machine interface and its interaction modalities.

A. Airspace and Voronoi-based sectorization

The airspace under consideration is modeled as a bounded two-dimensional spatial domain $\Omega \subset \mathbb{R}^2$ in which aircraft follow planned trajectories over time. Let $\mathcal{A} = \{1, \ldots, N\}$ denote the set of aircraft present within a given planning horizon. Each aircraft $i \in \mathcal{A}$ is associated with a continuous trajectory

$$\gamma_i : [t_i^{\mathrm{in}}, t_i^{\mathrm{out}}] \to \Omega, \tag{1}$$

where $\gamma_i(t)$ gives the spatial position of aircraft i at time t, and t_i^{in} and t_i^{out} denote its planned entry and exit times from the considered airspace. Trajectories may consist of piecewise-linear route segments connecting waypoints, reflecting standard flight planning structures. The aggregate set of trajectories defines the spatio-temporal traffic demand within Ω and forms the basis for estimating controller taskload and coordination complexity.

DAS consists of partitioning Ω into K operational sectors such that workload is balanced and coordination requirements remain manageable over time. Controller workload within a sector arises from monitoring aircraft, managing conflicts, and performing inter-sector coordination, and can be estimated as a function of the number of aircraft, trajectory interactions, and sector boundary crossings occurring within that region over time.

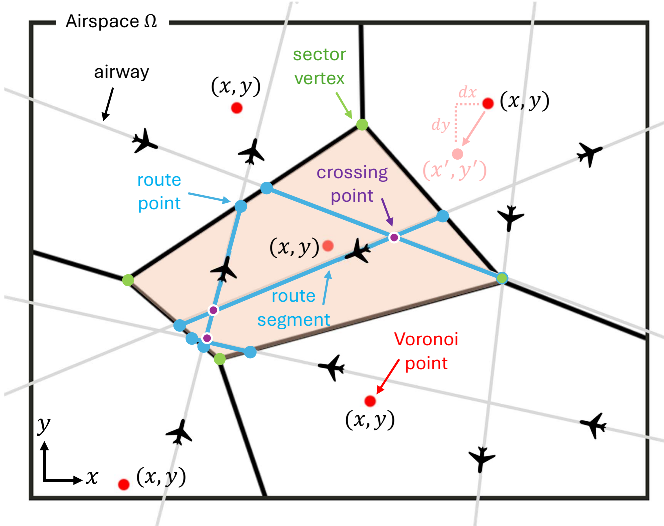

Figure 1. Airspace Voronoi tessellation.

To represent sector geometry in a form suitable for optimization and interaction, Voronoi tessellation is adopted as the underlying spatial model (see Figure 1). This representation naturally produces convex polygonal regions that align with common operational and geometric requirements for airspace sectors ([1], [2]). Let d denote the spatial dimension (typically $d = 2$). The optimization variable is the stacked vector of Voronoi center coordinates

$$\mathbf{x} \in \mathbb{R}^n, \qquad n = Kd, \qquad \mathbf{x} = [c_1^\top, c_2^\top, \ldots, c_K^\top]^\top, \tag{2}$$

where each $c_k \in \mathbb{R}^d$ represents the spatial position of sector center k. The Voronoi tessellation induced by these centers partitions the airspace according to nearest-center proximity:

$$V_k = \left\{ p \in \mathbb{R}^d : \|p - c_k\| \leq \|p - c_j\|, \ \forall j \neq k \right\}. \tag{3}$$

Each operational sector is defined as $S_k = V_k \cap \Omega$, ensuring complete coverage of the airspace through convex and contiguous regions.

This formulation is particularly well suited for human-in-the-loop optimization. Because sector geometry is fully determined by a small set of generator points, human operators can intuitively manipulate sector configurations by repositioning centers, immediately producing valid partitions without manually redrawing boundaries. Convexity and spatial continuity are preserved by construction, and incremental adjustments to center positions produce predictable changes in sector shape, workload distribution, and coordination structure. Combined with efficient computational construction methods such as Fortune's sweep-line algorithm [19], Voronoi-based sectorization provides a transparent and computationally efficient foundation for interactive optimization in which human judgment and algorithmic search can be tightly integrated.

B. Sector taskload modeling

Given the set of trajectories $\{\gamma_i\}$, aircraft are assigned dynamically to sectors according to their spatial position over time. Sector entry and exit events occur at times when a trajectory crosses sector boundaries, directly contributing to coordination workload and inter-sector hand-offs. The resulting sectorization therefore determines both the spatial distribution of traffic-related taskload and the temporal structure of coordination demands across sectors.

Sector complexity is evaluated over discrete time steps based on the distribution and dynamics of aircraft within each sector. Let $\mathcal{P}(t) = \{1, \ldots, N(t)\}$ denote the set of aircraft present in the airspace at time t, where each aircraft i has spatial position $\mathbf{p}_i(t) \in \Omega$. Let $\{S_k\}_{k=1}^K$ denote the set of sector polygons.

For each sector S_k, define the set of aircraft currently inside the sector:

$$\mathcal{I}_k(t) = \{ i \in \mathcal{P}(t) \mid \mathbf{p}_i(t) \in S_k \}. \tag{4}$$

The instantaneous number of aircraft within the sector is

$$N_k(t) = |\mathcal{I}_k(t)|. \tag{5}$$

Sector entries and exits are computed by comparing the current set of aircraft with the previous time step:

$$E_k(t) = |\mathcal{I}_k(t) \setminus \mathcal{I}_k(t-1)|, \tag{6}$$

$$X_k(t) = |\mathcal{I}_k(t-1) \setminus \mathcal{I}_k(t)|. \tag{7}$$

Additional complexity contributions arise from internal route crossings and conflict-related separation issues within the sector:

$$C_k(t) = \text{number of route crossings inside } S_k, \tag{8}$$

$$F_k(t) = \text{number of conflict events inside } S_k. \tag{9}$$

The total instantaneous complexity score for sector k at time t is then computed as a weighted sum [20]:

$$\Gamma_k(t) = w_p N_k(t) + w_{ee}\big(E_k(t) + X_k(t)\big) + w_c C_k(t) + w_f F_k(t), \tag{10}$$

where w_p, w_{ee}, w_c, and w_f are tunable weighting coefficients reflecting the relative contribution of aircraft count, coordination events, route crossings, and conflict-related workload to perceived controller complexity.

For each time step t, the vector of sector complexities is defined as

$$\boldsymbol{\Gamma}(t) = \big[\Gamma_1(t), \Gamma_2(t), \ldots, \Gamma_K(t)\big]. \tag{11}$$

From this vector, aggregate workload indicators across all sectors are computed to characterize the overall traffic management complexity at time t. The mean sector complexity is given by

$$\mu(t) = \frac{1}{K} \sum_{k=1}^{K} \Gamma_k(t), \tag{12}$$

and the corresponding standard deviation is

$$\sigma(t) = \sqrt{\frac{1}{K} \sum_{k=1}^{K} \big(\Gamma_k(t) - \mu(t)\big)^2}. \tag{13}$$

In addition, the minimum and maximum sector complexity values are recorded as

$$\Gamma_{\min}(t) = \min_k \Gamma_k(t), \tag{14}$$

$$\Gamma_{\max}(t) = \max_k \Gamma_k(t). \tag{15}$$

Over a time horizon $t \in [T_0, T_1]$, global indicators are obtained by aggregating across all time steps. The overall mean and standard deviation are computed from the flattened set of complexity values,

$$\mu_{\text{all}} = \frac{1}{KT} \sum_{t=T_0}^{T_1} \sum_{k=1}^{K} \Gamma_k(t), \tag{16}$$

$$\sigma_{\text{all}} = \sqrt{\frac{1}{KT} \sum_{t=T_0}^{T_1} \sum_{k=1}^{K} \big(\Gamma_k(t) - \mu_{\text{all}}\big)^2}, \tag{17}$$

where $T = T_1 - T_0 + 1$. The global minimum and maximum complexity values across all sectors and time steps are

$$\Gamma_{\min}^{\text{all}} = \min_{t,k} \Gamma_k(t), \tag{18}$$

$$\Gamma_{\max}^{\text{all}} = \max_{t,k} \Gamma_k(t). \tag{19}$$

Finally, the total number of inter-sector hand-offs over the considered time horizon is given by

$$H_{\text{tot}} = \sum_{t=T_0}^{T_1} \sum_{k=1}^{K} \big(E_k(t) + X_k(t)\big), \tag{20}$$

providing a direct measure of coordination workload induced by the sectorization.

C. Multi-objective CMA-ES

Two competing operational objectives are optimized within the proposed sectorization framework. The first objective promotes balanced controller workload across sectors by minimizing the dispersion of sector complexity values over time. Using the previously defined sector complexity $\Gamma_k(t)$, the time-averaged complexity per sector is

$$\overline{\Gamma}_k(x) = \frac{1}{T} \sum_{t=T_0}^{T_1} \Gamma_k(t; x), \tag{21}$$

where x denotes the vector of sector generator parameters and $T = T_1 - T_0 + 1$ is the number of evaluated time steps. The mean complexity across all sectors is

$$\overline{\Gamma}(x) = \frac{1}{K} \sum_{k=1}^{K} \overline{\Gamma}_k(x), \tag{22}$$

and workload balance is expressed through the standard deviation of sector complexity:

$$f_1(x) = \sigma_\Gamma(x) = \sqrt{\frac{1}{K} \sum_{k=1}^{K} \big(\overline{\Gamma}_k(x) - \overline{\Gamma}(x)\big)^2}. \tag{23}$$

Minimizing $f_1(x)$ promotes an equitable distribution of controller taskload across sectors.

The second objective captures coordination complexity through the total number of inter-sector hand-offs:

$$f_2(x) = H_{\text{tot}}(x) = \sum_{t=T_0}^{T_1} \sum_{k=1}^{K} \big(E_k(t; x) + X_k(t; x)\big), \tag{24}$$

where $E_k(t)$ and $X_k(t)$ denote aircraft entries and exits for sector k at time t. Lower values of $f_2(x)$ correspond to more continuous sector structures and reduced coordination workload between controllers.

Because these objectives are generally conflicting, a stochastic scalarization approach converts the multi-objective problem into a sequence of single-objective optimization problems [21]. At each optimization run, a random scalarization weight is sampled,

$$u \sim \mathcal{U}(0, 1), \qquad w^{(t)} = \begin{bmatrix} u \\ 1 - u \end{bmatrix}, \tag{25}$$

and the resulting scalarized objective becomes

$$J^{(t)}(x) = w_1^{(t)} \frac{f_1(x)}{s_1} + w_2^{(t)} \frac{f_2(x)}{s_2}, \tag{26}$$

where s_1 and s_2 are normalization constants. Varying the scalarization weights across runs enables exploration of different trade-offs between balanced sector complexity and reduced coordination workload.

Here, optimization is performed using the Covariance Matrix Adaptation Evolution Strategy (CMA-ES) [22], [23]. CMA-ES is a stochastic, derivative-free optimizer for continuous variables $\mathbf{x} \in \mathbb{R}^n$. At iteration t, a population of λ candidate solutions is sampled from a multivariate normal distribution

$$\mathbf{x}_{t,i} \sim \mathcal{N}(\mathbf{m}_t,\ \sigma_t^2 \mathbf{C}_t), \qquad i = 1, \ldots, \lambda, \tag{27}$$

where $\mathbf{m}_t$ is the current mean estimate, σ_t the global step size, and $\mathbf{C}_t$ the covariance matrix describing the search distribution. After evaluation, the best μ candidates ($\mu \leq \lambda$) are selected and recombined to update the mean:

$$\mathbf{m}_{t+1} = \sum_{i=1}^{\mu} \omega_i\, \mathbf{x}_{t,i:\lambda}, \qquad \sum_{i=1}^{\mu} \omega_i = 1, \quad \omega_i > 0, \tag{28}$$

where ω_i are positive recombination weights that determine the relative influence of each selected candidate. The notation $\mathbf{x}_{t,i:\lambda}$ denotes the i-th best candidate after ranking all λ samples. The covariance matrix and step size are subsequently adapted based on the distribution of successful search steps, allowing the sampling distribution to progressively concentrate around promising regions of the search space. Through iterative sampling, evaluation, and adaptation of $(\mathbf{m}_t, \sigma_t, \mathbf{C}_t)$, CMA-ES efficiently explores high-dimensional continuous spaces and converges toward sector configurations that optimize the defined performance objectives.

It is important to mention that CMA-ES assumes a *stationary* objective function to reliably adapt its search distribution across generations. If the scalarization weights are changed at every iteration, the effective objective function becomes non-stationary. As a consequence, the optimizer attempts to adapt its covariance matrix and step size to a constantly shifting landscape, which disrupts the statistical information accumulated from previous generations. This typically results in unstable search behavior, slower convergence, or premature convergence to suboptimal regions.

Note that DAS can in principle be addressed using a variety of alternative multi-objective optimization techniques, including evolutionary approaches such as NSGA-II [15], multi-objective particle swarm optimization (MOPSO) [24], or other heuristic search methods that directly approximate the Pareto frontier of trade-offs between workload balance and coordination complexity. However, the present problem is characterized by a continuous, high-dimensional decision space in which small geometric changes to sector boundaries can produce non-linear and non-smooth effects on complexity metrics. CMA-ES is particularly well suited to such settings because it adapts the full covariance structure of its sampling distribution, enabling efficient exploration of correlated and anisotropic search spaces without requiring gradient information. This makes it robust to the non-convex and noisy objective landscape induced by discrete aircraft movements and boundary-crossing events. Combined with stochastic scalarization to explore different trade-offs between objectives, which can be intuitively interpreted by humans, CMA-ES provides an effective and flexible optimization backbone for interactive, human-in-the-loop dynamic sectorization.

D. Human-Machine Interface

The sectorization HMI is organized into three tightly coupled views that support interactive and explainable sectorization design, see Figure 2. The *Environment* view displays the two-dimensional airspace, including airway structures, current sector boundaries, Voronoi center locations, and visual indicators of operational constraint violations such as route crossings too close to sector borders or excessively short route segments. Users can directly manipulate the sectorization by adding, removing, and dragging Voronoi centers to reshape sectors in real time. For finer geometric control, the interface also provides a "Polygon mode" that allows direct manipulation of sector polygon vertices, enabling local adjustments to resolve constraint violations or improve sector alignment with traffic flows (see Figure 3). A time slider further allows users to inspect predicted aircraft positions over time, providing temporal context for sector performance and constraint evaluation.

The *Chart* view presents predicted controller taskload information. When a specific sector is selected, the chart displays its predicted taskload evolution over time, including potential violations of maximum workload thresholds. During interactive manipulation of sectors—either through repositioning Voronoi centers or directly adjusting polygon vertices—the predicted taskload chart updates in real time, providing immediate feedback on the operational impact of geometric changes. If no sector is selected, the chart instead shows a stacked bar representation of taskload across all sectors for the currently selected time step, providing a system-wide overview of workload distribution and cross-sector standard deviation.

The *Pareto plot* visualizes candidate sectorization solutions generated by the CMA-ES optimization process in real time. Each point in the plot represents a complete sectorization configuration characterized by its workload balance and coordination complexity metrics. As the optimization progresses, the interface dynamically reveals the evolving solution set and highlights the Pareto front, enabling users to inspect trade-offs and select preferred Pareto-optimal configurations for further refinement or evaluation.

E. Human-in-the-loop interaction and solution steering

A typical sectorization workflow begins by selecting the number of Voronoi centers to correspond to the anticipated number of available ATCOs within the considered time horizon, thereby establishing the initial sector structure for subsequent refinement and optimization.

Subsequently, the operator iteratively refines the sector configuration to achieve a well-balanced distribution of taskload while maintaining operational feasibility. Initial Voronoi center positions can be adjusted manually or through the optimization process to reduce workload imbalances and minimize excessive inter-sector hand-offs. For the latter, a typical workflow would be as depicted in Figure 4:

1) *Start optimization*: By pressing the 'play' button, one can observe CMA-ES generate solutions and dynamically draw the Pareto front. During CMA-ES optimization, the changing sectorization topology can be observed in the Environment.
2) *Inspect sectorization solutions*: The optimization process can be stopped at any time or automatically stops when solutions do not change over at least 10 generations. Hovering the mouse cursor over solutions reveals the objectives trade-off and weights. Clicking a Pareto point will display the corresponding sectorization configuration in the Environment. Users can nudge or refine solutions manually by dragging Voronoi centers.
3) *Steer optimization*: By right clicking a Pareto point, a drop-down menu opens enabling CMA-ES to be restarted from the layout corresponding to that Pareto point.
4) *Restart*: Restarting CMA-ES will generate new solutions around the selected sectorization configurations.

Restarting the optimization from a configuration replaces the CMA-ES mean vector $\mathbf{m}_t$ with the chosen Voronoi center vector, thereby centering subsequent search around the user-approved sectorization. Alternatively, user-provided sector centers can be injected directly to override or bias the search distribution, either by fully redefining $\mathbf{m}_t$ or by blending the current mean with human-proposed centers using a convex combination. This interactive mechanism allows the algorithm to retain its adaptive exploration capabilities while incorporating expert judgment, enabling iterative refinement of sectorization solutions that remain both computationally efficient and operationally aligned with human expectations.

IV. Human Preference Meta-Learner

Beyond direct human interaction mechanisms such as freezing the optimization, revising sectorizations, selecting Pareto-optimal solutions, or restarting the search from user-defined configurations, the human operator can also provide explicit qualitative feedback by labeling generated sectorizations as *preferred* or *to be avoided* (see Figure 4). These binary annotations constitute an additional optimization signal that complements the intrinsic performance objectives (e.g. workload balance or hand-off minimization) and can be incorporated as a learned preference-based target shaping the search process. Rather than replacing the base objective, such

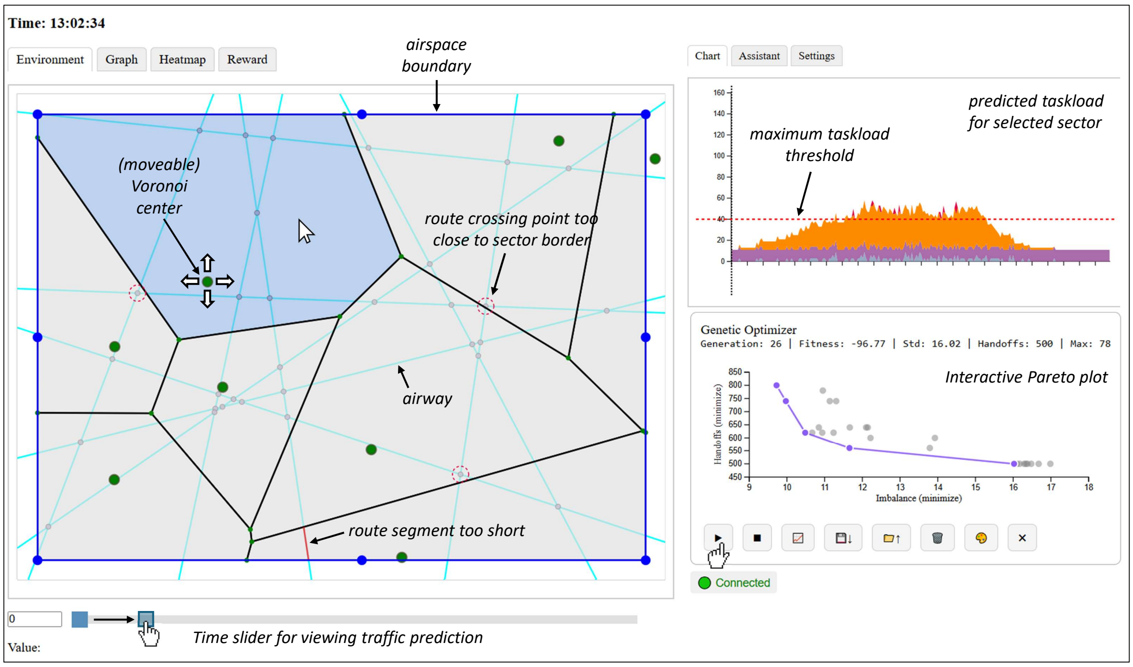

Figure 2. HMI for airspace sectorization. Demo available at: https://github.com/clarkborst/ATMSectorization

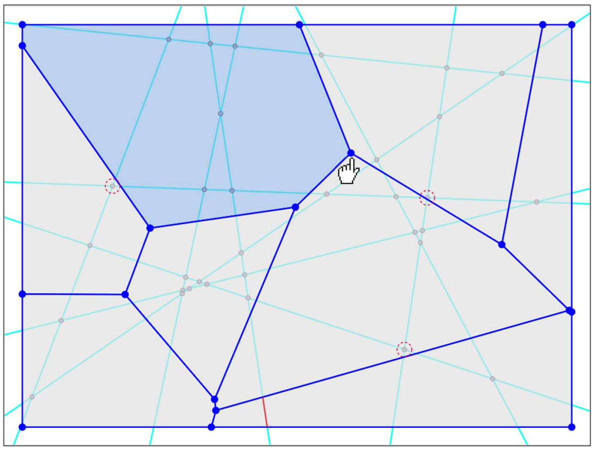

Figure 3. Polygon edit mode, allowing direct manipulation of sector polygon vertices.

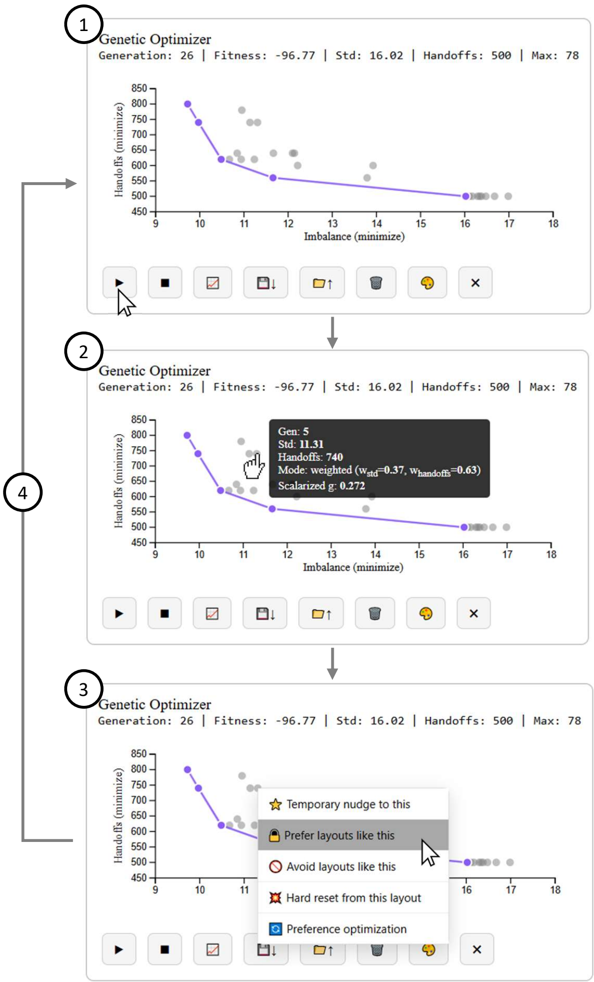

Figure 4. Human-in-the-loop interaction and solution steering.

feedback augments it, allowing the optimizer to progressively align with human operational intent while preserving its ability to explore novel configurations.

Let $\mathbf{x} \in \mathbb{R}^{2n}$ denote the vectorized coordinates of n Voronoi centers defining a candidate sectorization layout, where each pair of entries represents the spatial coordinates of one center and therefore the full vector uniquely specifies a complete airspace partition. At generation t, the optimizer evaluates an intrinsic task-specific cost $J(\mathbf{x})$ representing operational metrics such as workload imbalance, coordination complexity, or predicted controller taskload dispersion. In parallel, the human feedback module computes a real-time preference reward $R(\mathbf{x}, t)$ derived from labeled sectorizations. The combined scalarized objective guiding optimization is

$$F(\mathbf{x}, t) = J(\mathbf{x}) - \alpha(t)\, R(\mathbf{x}, t), \tag{29}$$

where $F(\mathbf{x}, t)$ is the augmented objective minimized by CMA-ES, $R(\mathbf{x}, t)$ is the learned preference reward representing the degree of human approval, and $\alpha(t) \geq 0$ is a time-dependent weighting factor controlling how strongly human guidance influences the search. In CMA-ES this objective is minimized directly, while in genetic algorithms the same expression may be interpreted as a maximized fitness. The preference reward combines continuous kernel-based influence from labeled samples and optional relational preference comparisons.

Each labeled configuration $\mathbf{x}_i$ is associated with a human label $y_i \in \{+1, -1\}$, where $+1$ indicates a preferred configuration and -1 indicates a configuration to be avoided. Every labeled sample induces a Gaussian kernel in the configuration space, producing a smooth reward field:

$$R_{\text{kernel}}(\mathbf{x}) = \frac{1}{Z} \sum_i y_i \exp\left[-\frac{\|\mathbf{x} - \mathbf{x}_i\|^2}{2\sigma^2}\right], \tag{30}$$

where $\|\mathbf{x} - \mathbf{x}_i\|$ denotes Euclidean distance between the current configuration and labeled sample i, σ is the kernel width controlling spatial influence of each sample, and Z is a normalization constant ensuring bounded reward magnitude. The exponential kernel produces positive reward near preferred samples and negative reward near rejected samples, yielding a smooth landscape that biases exploration toward human-aligned regions while preserving continuity. Optionally, each contribution may be multiplied by a temporal decay factor $e^{-(t-t_i)/\tau}$, where t_i is the labeling time and τ controls how quickly older feedback becomes less influential.

The influence of human feedback can be gradually increased through a ramp-up schedule:

$$\alpha(t) = \alpha_{\min} + (\alpha_{\max} - \alpha_{\min}) \left(\frac{t}{T_{\max}}\right)^{\gamma}, \tag{31}$$

where $\alpha_{\min}$ and $\alpha_{\max}$ define minimum and maximum preference influence, $T_{\max}$ is the total number of generations, and $\gamma > 1$ produces a nonlinear ease-in schedule. Early iterations emphasize exploration of the intrinsic objective J, whereas later iterations increasingly exploit regions aligned with human preferences.

To further enhance adaptability, the meta-learner adjusts its spatial sensitivity through online meta-learning of kernel parameters. For a candidate configuration represented by Voronoi centers $\mathbf{x}$ and a labeled sample $(\mathbf{x}_i, y_i)$, the contribution of that sample is

$$r_i(\mathbf{x}) = y_i \exp\left(-\frac{D^2(\mathbf{x}, \mathbf{x}_i)}{2\sigma^2}\right), \tag{32}$$

where $D(\mathbf{x}, \mathbf{x}_i)$ denotes the average Euclidean distance between corresponding centers and σ is the kernel width controlling spatial generalization. The normalized kernel reward becomes

$$R_{\text{kernel}}(\mathbf{x}) = \frac{\sum_i r_i(\mathbf{x})}{\sum_i \exp\left(-\frac{D^2(\mathbf{x}, \mathbf{x}_i)}{2\sigma^2}\right)}, \tag{33}$$

ensuring bounded and scale-consistent reward magnitude between $[-1, 1]$. To adapt σ automatically, the system evaluates consistency of recent feedback. Let the most recent k labeled samples be $\{(\mathbf{x}_t, y_t)\}_{t=T-k}^{T}$ with labels $y_t \in \{+1, -1\}$. The consistency metric is

$$\kappa = \frac{1}{k-1} \sum_{i=T-k+1}^{T} y_i y_{i-1} \exp\left(-\frac{D^2(\mathbf{x}_i, \mathbf{x}_{i-1})}{2\sigma^2}\right), \tag{34}$$

where $\kappa > 0$ indicates consistent preferences in nearby regions and $\kappa < 0$ indicates contradictory feedback. The kernel width adapts according to

$$\sigma \leftarrow \begin{cases} \sigma(1 - \zeta), & \text{if } \kappa > 0, \\ \sigma(1 + 0.5\zeta), & \text{if } \kappa \leq 0, \end{cases} \tag{35}$$

where ζ is a small meta-learning rate. Consistent feedback narrows the spatial generalization to focus on local refinement (exploitation), whereas inconsistent feedback broadens spatial generalization (exploration). The overall preference influence weight may also adapt:

$$\omega \leftarrow \omega(1 + \beta \max(0, \kappa)), \tag{36}$$

where β controls how strongly consistent feedback increases global human influence.

Human preferences can be interpreted as shaping a reward landscape over the continuous space of sector generator parameters. In particular, user preferences can be directly mapped to preferred Voronoi center locations using Equation (30), allowing the system to portray a spatial reward field within the Environment that reflects desirable regions of the solution space (see Figure 5). This reward landscape highlights configurations that better align with human judgment, operational intuition, and constraint satisfaction. As a result, the optimization process can be guided toward these regions, with sampled sectorization solutions progressively drawn toward areas of higher inferred reward areas shown in shades of green. In this way, human feedback is translated into a structured preference signal that informs and steers the search process while preserving transparency and interpretability.

Finally, preferred solutions can be saved to and loaded from a JSON file, enabling ATCOs to access their personal profiles and/or retrieve favorable solutions from a shared database to 'warm start' the optimization process.

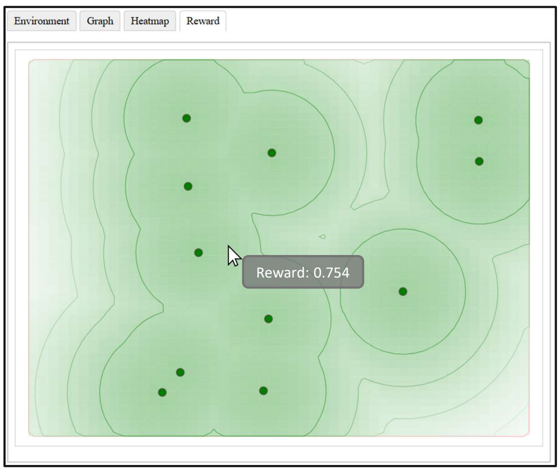

Figure 5. Human-preference reward landscape.

V. System Interoperability

The current system already incorporates the embedded multi-objective CMA-ES optimization engine and preference learner that can generate and guide candidate sectorizations and support interactive exploration of trade-offs between competing objectives. To facilitate integration with other external tools and research platforms, the sectorization system has been designed with an interoperability layer that supports communication through lightweight JSON-based messaging. This architecture enables external modules, optimization engines, or visualization tools to interface with the system using Python or any other programming language capable of sending and receiving structured JSON messages.

The system itself is implemented as a browser-based JavaScript/HTML application that serves as the primary human–machine interface. Interoperability is achieved through a WebSocket-based communication layer that allows bidirectional exchange of JSON messages between the interface and external processes. The application listens on port `8765` for incoming JSON messages and uses the same channel to transmit responses back to connected external modules. In this configuration, the JavaScript application acts as the frontend client, while an external Python script would typically function as the backend server responsible for optimization, simulation, or data processing tasks.

Through this WebSocket connection, external Python processes can send JSON-encoded commands to update sector geometries, display messages, trigger optimization steps, or request specific visualizations within the interface. Conversely, the JavaScript application continuously monitors incoming messages, executes the corresponding actions, and returns JSON-formatted reports containing sector configurations, constraint violations, and workload metrics. This bidirectional messaging framework enables synchronization between the interactive interface and external computational modules. The use of language-agnostic JSON messaging and standard WebSocket communication ensures flexibility, allowing researchers and developers to integrate the system within diverse experimental pipelines, optimization frameworks, or operational prototypes without dependency on a specific software stack.

VI. Operational Use Case

Within the context of the AI4REALNET EU project, the sectorization application has been developed using an operationally motivated use case provided by NAV Portugal, the Air Navigation Service Provider (ANSP) of Portugal. The focus lies on the Santa Maria oceanic airspace, where controllers face substantial coordination workload due to the large geographical extent of the Flight Information Region (FIR) and the characteristics of transatlantic traffic flows. In addition to existing operational complexity, NAV Portugal anticipates future challenges related to staffing constraints, evolving communication infrastructures, and environmental considerations. In particular, expected shortages in available ATCOs require sector configurations that can flexibly adapt to reduced staffing levels while maintaining safe and balanced workload distributions. At the same time, environmental objectives such as the avoidance of contrail-sensitive regions and improved weather and climate adaptation strategies are becoming increasingly important.

Current reliance on high-frequency (HF) communication in oceanic airspace introduces further operational limitations due to noise, latency, and vulnerability to atmospheric disturbances. As part of modernization efforts, NAV Portugal is exploring the transition toward satellite-based VHF communication to improve reliability and clarity. However, satellite-based VHF introduces its own constraints, including limited communication channels that may restrict how sectors can be configured and managed. These combined factors motivate the need for advanced sectorization support tools capable of exploring the impact of staffing levels, communication limitations, and environmental constraints on airspace design.

The proposed sectorization assistant enables exploratory analysis of such scenarios by allowing users to perform interactive "what-if" investigations as illustrated in Figure 6. The system accepts planned flight trajectories as input, including entry times into the FIR and route waypoints, together with FIR boundary definitions. Users can introduce disturbances in the form of static polygonal regions representing areas to be avoided, such as contrail-sensitive zones, regions with limited satellite-based VHF coverage, and/or weather-related perturbations. Once disturbances are defined, an integrated any-angle pathfinding algorithm based on Theta* [25] automatically re-plans affected trajectories to avoid these regions while maintaining feasible and shortest-path routing to avoid excessive flight delays.

The resulting changes in traffic patterns may significantly alter spatial and temporal workload distributions, thereby requiring revised sectorization strategies. By coupling trajectory replanning with interactive sector design and optimization, the application allows airspace designers to visually assess the operational consequences of different scenarios. Users can evaluate predicted taskload per sector, cross-sector workload balance, and coordination workload in real time, enabling informed decision-making about sector configurations under evolving staffing, environmental, and communication constraints.

VII. Future Work and Outlook

The current sectorization system represents an initial fully integrated research prototype aimed at demonstrating the feasibility and value of human participation in DAS through a shared human–algorithm design framework. A central goal of the developed system is to establish a common ground for sectorization in which both human operators and optimization algorithms operate under the same action-relevant constraints and performance metrics. Within this shared environment, humans can either manually construct suitable sectorizations or be supported by algorithmic optimization methods, while retaining full transparency over constraint satisfaction and operational trade-offs. By ensuring that both human and computational agents have access to and can perceive the same work domain and constraint structures, the system enables seamless collaboration and informed co-adaptation

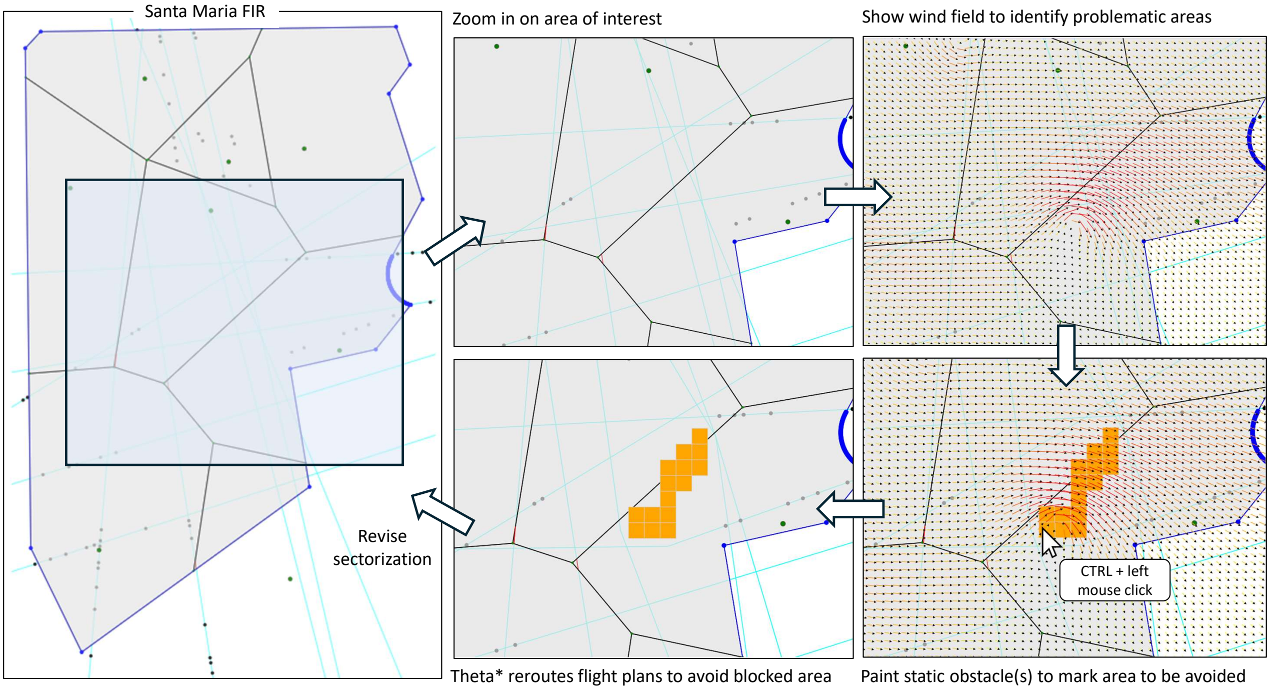

Figure 6. Operational use case for the Santa Maria FIR. Wind data are loaded as speed vectors at discrete spatial locations and visualized as a vector field, where arrows indicate wind direction and magnitude while color coding represents wind speed intensity.

between manual design and automated optimization. Future work will focus on evaluating and extending this collaborative approach in close cooperation with operational stakeholders while maintaining the mathematical foundations that underpin the system.

A primary next step is the execution of a structured human-in-the-loop evaluation with operational experts from NAV Portugal. These experiments will assess system usability, operator acceptance, and the practical viability of meaningful human participation in the optimization process. In particular, the evaluation will examine how effectively airspace designers and supervisors can interact with the system, interpret optimization trade-offs, and guide sectorization toward operationally acceptable solutions.

Beyond performance outcomes, a central focus will be on understanding how human users adapt and refine algorithm-generated sectorizations, and whether recurring adjustment patterns reveal tacit operational knowledge not explicitly captured in the current objective functions. For instance, operators may consistently align sector boundaries with dominant traffic flows to minimize coordination effort, or avoid geometrically optimal configurations that appear fragile under minor traffic perturbations.

In addition to geometric considerations, explicitly incorporating ATCo assignment to sectors offers a mechanism for capturing such tacit knowledge. By enabling users to associate controller expertise levels with individual polygons, the system can record implicit judgments about sector complexity that are otherwise difficult to formalize. These annotations provide insight into how practitioners balance workload against human capability, thereby bridging the gap between quantitative optimization metrics and operational reasoning. Over time, this information could be leveraged to inform human-aware optimization models or to learn mappings between sector characteristics and required controller expertise.

By logging and analyzing these interaction patterns, the study aims to identify consistent human strategies that can inform future extensions of the optimization framework. Furthermore, the evaluation will investigate whether the interface supports exploratory *what-if* analyses, enabling NAV Portugal to anticipate and prepare for evolving operational conditions, such as changes in staffing levels, communication infrastructures, and environmental constraints. Finally, the study will assess whether active human involvement enhances trust in, and acceptance of, algorithmic recommendations.

From a technical perspective, future development will extend the current two-dimensional sectorization model toward a three-dimensional representation of the airspace. This includes incorporating altitude as an explicit design dimension by modeling sectors as stacked vertical layers covering specified flight level ranges [15], [26], [27]. Such an extension will enable more realistic representation of operational sector structures and allow exploration of vertical sectorization strategies alongside horizontal boundary adjustments. While the introduction of richer and more realistic flight trajectories and operational data will increase fidelity, the underlying mathematical modeling of sector complexity, workload balancing, and optimization over continuous sector parameters remains valid and directly extensible to these enhanced scenarios.

Finally, the system will be expanded to support richer data integration from external operational sources. Planned enhancements include the incorporation of meteorological data, higher-fidelity flight plan and trajectory prediction models, controller staffing schedules, and communication infrastructure constraints. Integrating these data sources will enable more realistic simulation of operational conditions and allow sectorization proposals to be evaluated against a broader set of constraints and uncertainties. By combining human-centered interaction, advanced optimization, and integrated operational data, the envisioned system aims to evolve into a comprehensive decision-support environment for exploring and designing future airspace sectorization concepts.

ACKNOWLEDGEMENTS

The author would like to express sincere gratitude to the operational experts at NAV Portugal for their valuable guidance, domain expertise, and continuous feedback throughout the development of the sectorization prototype. Their insights into operational procedures, constraints, and future challenges in oceanic ATM have been instrumental in shaping the design and functionality of the system.

REFERENCES

[1] D. Delahaye, M. Schoenauer, and J.-M. Alliot, "Airspace Sectoring by Evolutionary Computation," in *1998 IEEE International Conference on Evolutionary Computation Proceedings*, pp. 218–223, 06 1998.

[2] M. Xue, "Airspace Sector Redesign Based on Voronoi Diagrams," *Journal of Aerospace Computing, Information, and Communication*, vol. 6, no. 12, pp. 624–634, 2009.

[3] M. Schultz, I. Gerdes, T. Standfuß, and A. Temme, "Future Airspace Design by Dynamic Sectorization," in *Air Traffic Management and Systems III*, (Singapore), pp. 19–34, Springer Singapore, 2019. Lecture Notes in Electrical Engineering.

[4] I. Gerdes, A. Temme, and M. Schultz, "Dynamic Airspace Sectorisation for Flight-Centric Operations," *Transportation Research Part C: Emerging Technologies*, vol. 95, pp. 460–480, 2018.

[5] N. Ahrenhold, I. Gerdes, T. Mühlhausen, and A. Temme, "Validating Dynamic Sectorization for Air Traffic Control Due to Climate Sensitive Areas: Designing Effective Air Traffic Control Strategies," *Aerospace*, vol. 10, no. 5, 2023.

[6] National Academies of Sciences, Engineering, and Medicine, "The Air Traffic Controller Workforce Imperative: Strategies for Sustainable Staffing," tech. rep., The National Academies Press, Washington, DC, 2025. doi: 10.17226/27533.

[7] A. A. Hijosa, M. M. Martínez, J. L. C. García, M. G. Martín, J. M. G. Cano, and D. F. Fernandez, "Space-Based VHF, a Bridge to the Future," in *2025 Integrated Communications, Navigation and Surveillance Conference (ICNS)*, pp. 1–8, 2025. doi:10.1109/ICNS65417.2025.10976867.

[8] M. Addala, A. Mogtit, and M. Lagha, "A Chronological Review of Airspace Sectorization Approaches Applied to Enhancing Air Traffic Management," *Aircraft Engineering and Aerospace Technology*, vol. 97, pp. 1200–1218, 09 2025. https://doi.org/10.1108/AEAT-04-2024-0123.

[9] J. Schon, C. Bruder, M. Liebherr, and S. Theis, "Cleared for Takeoff - Artificial Intelligence Acceptance in Air Traffic Control," *Proceedings of the 4th Annual Symposium on Human-Computer Interaction for Work*, 2025. https://api.semanticscholar.org/CorpusID:279453488.

[10] European Union Aviation Safety Agency, "The EASA AI Roadmap 2.0: A deliverable of the EASA Artificial Intelligence Programme," tech. rep., EASA, Cologne, Germany, May 2023. https://www.easa.europa.eu.

[11] European Union, "Regulation (EU) 2024/1689 of the European Parliament and of the Council of 13 June 2024 laying down harmonised rules on artificial intelligence (Artificial Intelligence Act): Article 14: Human Oversight," 2024. https://eur-lex.europa.eu/eli/reg/2024/1689/oj.

[12] C. Gómez Arnaldo, J. M. Arroyo López, *et al.*, "Airspace Sector Design: An Optimization Approach," in *Proceedings of the SESAR Innovation Days (SIDs 2024)*, (Rome, Italy), November 2024. https://research.lancaster-university.uk/en/publications/airspace-sector-design-an-optimization-approach/.

[13] T. A. Granberg, T. Polishchuk, V. Polishchuk, and C. Schmidt, "Integer Programming–Based Airspace Sectorization for Terminal Maneuvering Areas with Convex Sectors," *Journal of Air Transportation*, vol. 27, no. 4, pp. 169–180, 2019.

[14] M. Sergeeva, D. Delahaye, C. Mancel, and A. Vidosavljevic, "Dynamic Airspace Configuration by Genetic Algorithm," *Journal of Traffic and Transportation Engineering (English Edition)*, vol. 4, no. 3, pp. 300–314, 2017.

[15] W. Zhang, M. Hu, J. Yin, H. Li, and J. Du, "Multi-Objective 3D Airspace Sectorization Problem Using NSGA-II with Prior Knowledge and External Archive," *Aerospace*, vol. 10, no. 3, 2023.

[16] M. Melgosa, A. Vidosavljevic, and X. Prats, "Hybrid Method for Holistic Air Traffic Demand and Capacity Balancing Optimisation Based on Sector Complexity," *Transportation Research Part C: Emerging Technologies*, vol. 180, p. 105306, 2025. https://doi.org/10.1016/j.trc.2025.105306.

[17] T. Zhao, J. Escribano, A. Majumdar, and W. Y. Ochieng, "Robust 3D Dynamic Airspace Sectorization: A Multilayer Graph-Based Approach," *Journal of Air Transport Management*, vol. 132, p. None, None 2026. 10.1016/j.jairtraman.2025.102953.

[18] W. Zhou, D.-T. Pham, and S. Alam, "AirFusion: A Machine Learning Framework for Balancing Air Traffic Demand and Airspace Capacity Through Dynamic Airspace Sectorization," in *2023 IEEE 26th International Conference on Intelligent Transportation Systems (ITSC)*, pp. 5324–5331, 2023.

[19] S. Fortune, "A Sweepline Algorithm for Voronoi Diagrams," *Algorithmica*, vol. 2, no. 1, pp. 153–174, 1987.

[20] J. Li, T. Wang, M. Savai, and I. Hwang, "Graph-Based Algorithm for Dynamic Airspace Configuration," *Journal of Guidance, Control, and Dynamics*, vol. 33, no. 4, pp. 1082–1094, 2010.

[21] B. Paria, K. Kandasamy, and B. Poczos, "A Flexible Multi-Objective Bayesian Optimization Approach using Random Scalarizations," 05 2018. https://arxiv.org/abs/1805.12168.

[22] N. Hansen and A. Ostermeier, "Completely Derandomized Self-Adaptation in Evolution Strategies," *Evolutionary Computation*, vol. 9, no. 2, pp. 159–195, 2001. 10.1162/106365601750190398.

[23] N. Hansen, "The CMA Evolution Strategy: A Comparing Review," *Towards a New Evolutionary Computation*, pp. 75–102, 2006. doi: 10.1007/3-540-32494-1_4.

[24] A. Chandra, S. Hazra, A. Verma, and K. Sooraj, "On the Possibilities of Efficient Air Traffic Monitoring through Complex Network Clustering Based Airspace Sub-Sectorization: A Multi-Objective Discrete Particle Swarm Optimization Approach," *Transportation Research Record*, vol. 2679, no. 2, pp. 2127–2143, 2025.

[25] K. Daniel, A. Nash, S. Koenig, and A. Felner, "Theta*: Any-Angle Path Planning on Grids," *Journal of Artificial Intelligence Research*, vol. 39, p. 533–579, Sept. 2010. https://dl.acm.org/doi/10.5555/1946417.1946429.

[26] M. Xue, "Three Dimensional Sector Design with Optimal Number of Sectors," in *AIAA Guidance, Navigation, and Control Conference*, pp. 1–16, 2010. https://arc.aiaa.org/doi/abs/10.2514/6.2010-8290.

[27] T. Zhao, J. Escribano, A. Majumdar, and W. Y. Ochieng, "Robust 3d dynamic airspace sectorization: A multilayer graph-based approach," *Journal of Air Transport Management*, vol. 132, 2026. https://doi.org/10.1016/j.jairtraman.2025.102953.